

# Self and Nonself Recognition of Asymmetric Catalysts. Nonlinear Effects in the Amino Alcohol-Promoted Enantioselective Addition of Dialkylzincs to Aldehydes

Masato Kitamura, Seiji Suga, Makoto Niwa, and Ryoji Noyori\*

Contribution from the Department of Chemistry, Nagoya University, Chikusa, Nagoya 464-01, Japan

Received January 3, 1995<sup>⊗</sup>

**Abstract:** Chiral  $\beta$ -dialkylamino alcohols promote enantioselective alkylation of aldehydes by dialkylzincs, where a tricoordinate alkylzinc aminoalkoxide in equilibrium with its dimer acts as a true catalyst. The presence of other aminoalkoxides causes nonlinear effects on the rate and stereoselectivity of the enantioselective catalysis. This is a general phenomenon where the extent of the departure from the linearity is highly affected by the nature of the amino alcohols. Systematic investigation using (2*S*)-3-*exo*-(dimethylamino)isoborneol and its stereoisomers as well as achiral 2-(dimethylamino)-1,1-dimethylethanol has revealed that the self and nonself recognition of the asymmetric catalysts are the major source of this unusual phenomena. The relative significance of these recognitions affects the overall profile of asymmetric catalysis.

Molecules in solution cannot exist independently but interact reversibly with the surrounding molecules not only solvents but also certain solute species. These pairs may have the same, similar, or entirely different properties. Intermolecular interaction that is sterically and electronically complementary in nature sometimes occurs with high selectivity, affecting the static and dynamic properties of the chemical entities to a great extent. Chirality plays an important role in such molecular recognition.<sup>1,2</sup> For instance, the solubility,<sup>2,3</sup> rotation,<sup>4</sup> NMR spectra,<sup>5</sup> and chromatographic behavior<sup>6</sup> of chiral compounds are highly influenced by enantiomeric purity. Our recent work<sup>7-9</sup> revealed that the self and nonself recognition of asymmetric catalysts result in a remarkable amplification of chirality.<sup>10</sup> Thus certain chiral  $\beta$ -dialkylamino alcohols catalyze the enantioselective

addition of dialkylzincs to benzaldehyde, giving after aqueous workup highly enantiomerically pure secondary alcohols, where the use of an enantiomerically pure amino alcohol and partially resolved compounds provide the alkylation products with equally high enantiomeric purities.<sup>1,7-9,11,12</sup> The origin of this unusual nonlinear effect was elucidated to be the diastereomeric interaction of chiral alkylzinc alkoxides that act as asymmetric catalysts.<sup>1,7-9</sup> We here disclose the more general implications of such effects in asymmetric catalysis.<sup>13-15</sup> This study examines the rate and enantioselectivity of the reaction promoted by a stereochemically impure or, more generally, chemically impure catalyst.

## General Consideration

First, suppose that an *S* catalyst promotes the enantioselective reaction of an achiral substrate leading to an enantiomerically

\* Abstract published in *Advance ACS Abstracts*, April 15, 1995.

(1) Noyori, R. *Asymmetric Catalysis in Organic Synthesis*; John Wiley & Sons: New York, 1994; Chapter 5.

(2) Jacques, J.; Collet, A.; Wilen, S. H. *Enantiomers, Racemates, and Resolutions*; John Wiley & Sons: New York, 1981.

(3) (a) van Mil, J.; Addadi, L.; Gati, E.; Lahav, M. *J. Am. Chem. Soc.* **1982**, *104*, 3429. (b) Addadi, L.; Berkovitch-Yellin, Z.; Weissbuch, I.; van Mil, J.; Shimon, L. J. W.; Lahav, M.; Leiserowitz, L. *Angew. Chem., Int. Ed. Engl.* **1985**, *24*, 466. (c) Fogassy, E.; Faigl, F.; Acs, M. *Tetrahedron Lett.* **1981**, *22*, 3093. (d) Fogassy, E.; Faigl, F.; Acs, M. *Tetrahedron* **1985**, *41*, 2841.

(4) (a) Horeau, A. *Tetrahedron Lett.* **1969**, 3121. (b) Horeau, A.; Guetté, J. P. *Tetrahedron* **1974**, *30*, 1923.

(5) (a) Williams, T.; Pitcher, R. G.; Bommer, P.; Gutzwiller, J.; Uskoković, M. *J. Am. Chem. Soc.* **1969**, *91*, 1871. (b) Harger, M. J. P. *J. Chem. Soc., Perkin Trans. II* **1977**, 1882. (c) Harger, M. J. P. *J. Chem. Soc., Perkin Trans. II* **1978**, 326. (d) Dobashi, A.; Saito, N.; Motoyama, Y.; Hara, S. *J. Am. Chem. Soc.* **1986**, *108*, 307. (e) Giordano, C.; Restelli, A.; Villa, M.; Annunziata, R. *J. Org. Chem.* **1991**, *56*, 2270. (f) Hong, C. Y.; Kishi, Y. *J. Am. Chem. Soc.* **1992**, *114*, 7001. (g) Pirkle, W. H.; Hoover, D. J. *Top. Stereochem.* **1982**, *13*, 316. (h) Shanzer, A.; Libman, J.; Gottlieb, H. E. *J. Org. Chem.* **1983**, *48*, 4612. (i) Luchinat, C.; Roelens, S. *J. Am. Chem. Soc.* **1986**, *108*, 4873.

(6) (a) Cundy, K. C.; Crooks, P. A. *J. Chromatogr.* **1983**, *281*, 17. (b) Charles, R.; Gil-Av, E. *J. Chromatogr.* **1984**, *298*, 516. (c) Tsai, W.-L.; Hermann, K.; Hug, E.; Rohde, B.; Dreiding, A. S. *Helv. Chim. Acta* **1985**, *68*, 2238. (d) Matusch, R.; Coors, C. *Angew. Chem., Int. Ed. Engl.* **1989**, *28*, 626.

(7) Noyori, R.; Suga, S.; Kawai, K.; Okada, S.; Kitamura, M. *Pure Appl. Chem.* **1988**, *60*, 1597.

(8) Kitamura, M.; Okada, S.; Suga, S.; Noyori, R. *J. Am. Chem. Soc.* **1989**, *111*, 4028.

(9) Noyori, R.; Kitamura, M. *Angew. Chem., Int. Ed. Engl.* **1991**, *30*, 49.

(10) (a) Mason, S. *Chem. Soc. Rev.* **1988**, *17*, 347. (b) Bonner, W. A. *Top. Stereochem.* **1988**, *18*, 1.

(11) Oguni, N.; Matsuda, Y.; Kaneko, T. *J. Am. Chem. Soc.* **1988**, *110*, 7877.

(12) (a) Bolm, C.; Schlingloff, G.; Harms, K. *Chem. Ber.* **1992**, *125*, 1191. (b) Bolm, C.; Müller, J.; Schlingloff, G.; Zehnder, M.; Neuburger, M. *J. Chem. Soc., Chem. Commun.* **1993**, 182. (c) Bolm, C.; Müller, J. *Tetrahedron* **1994**, *50*, 4355.

(13) Pioneering findings of chirality amplification effects: Puchot, C.; Samuel, O.; Duñach, E.; Zhao, S.; Agami, C.; Kagan, H. B. *J. Am. Chem. Soc.* **1986**, *108*, 2353. See also, Guillaneux, D.; Zhao, S.-H.; Samuel, O.; Rainford, D.; Kagan, H. B. *J. Am. Chem. Soc.* **1994**, *116*, 9430.

(14) For related chirality amplifying reactions, see: (a) Mikami, K.; Terada, M. *Tetrahedron* **1992**, *48*, 5671. (b) Terada, M.; Mikami, K. *J. Chem. Soc., Chem. Commun.* **1994**, 833. (c) Mikami, K.; Motoyama, Y.; Terada, M.; *J. Am. Chem. Soc.* **1994**, *116*, 2812. (d) Hayashi, M.; Matsuda, T.; Oguni, N. *J. Chem. Soc., Chem. Commun.* **1990**, 1364. (e) Bolm, C.; Ewald, M.; Felder, M. *Chem. Ber.* **1992**, *125*, 1205. (f) Tanaka, K.; Matsui, J.; Suzuki, H. *J. Chem. Soc., Perkin Trans. I* **1993**, 153. (g) Rossiter, B.; Eguchi, M.; Miao, G.; Swingle, N. M.; Hernández, A. E.; Vickers, D.; Fluckiger, E.; Patterson, R. G.; Reddy, K. V. *Tetrahedron* **1993**, *49*, 965. (h) Zhou, Q.-L.; Pfaltz, A. *Tetrahedron* **1994**, *50*, 4467. (i) de Vries, A. H. M.; Jansen, J. F. G. A.; Feringa, B. L. *Tetrahedron* **1994**, *50*, 4479. (j) Kobayashi, S.; Ishitani, H.; Araki, M.; Hachiya, I. *Tetrahedron Lett.* **1994**, *35*, 6325.

(15) (a) Iwasawa, N.; Hayashi, Y.; Sakurai, H.; Narasaka, K. *Chem. Lett.* **1989**, 1581. (b) Keck, G. E.; Krishnamurthy, D.; Grier, M. *J. Org. Chem.* **1993**, *58*, 6543. (c) Evans, D. A.; Nelson, S. G.; Gagné, M. R.; Muci, A. R. *J. Am. Chem. Soc.* **1993**, *115*, 9800. (d) Komatsu, N.; Hashizume, M.; Sugita, T.; Uemura, S. *J. Org. Chem.* **1993**, *58*, 4529. (e) Sasaki, H.; Suzuki, T.; Itoh, N.; Shibasaki, M. *Tetrahedron Lett.* **1993**, *34*, 851.

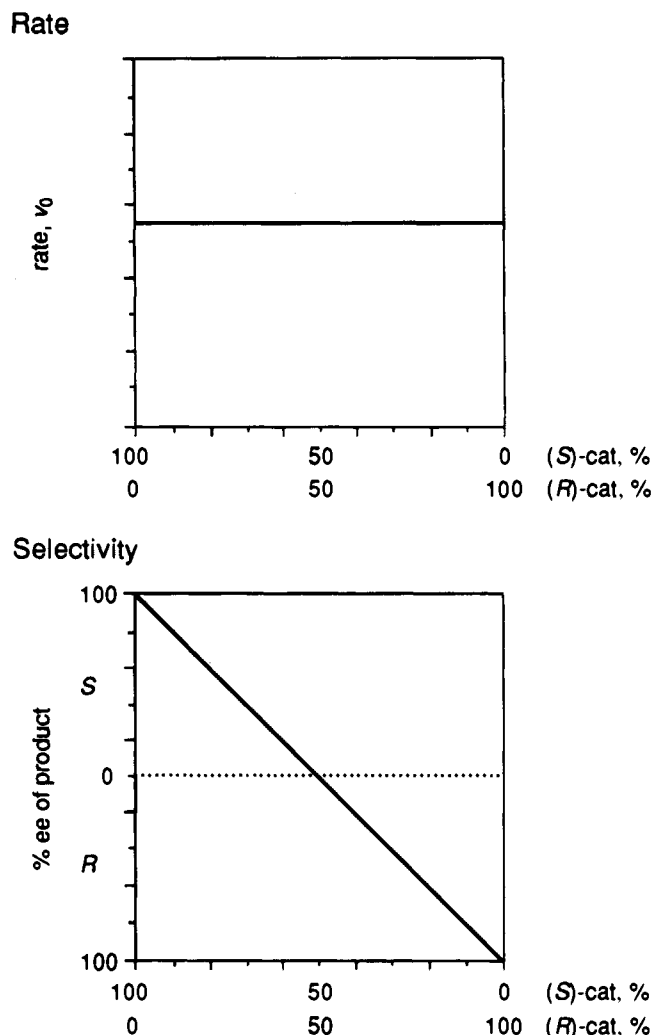
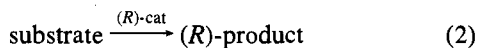
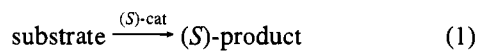


**Figure 1.** Linear relationship in enantioselective catalysis. Initial reaction rate and enantioselectivity as a function of the composition of the enantiomeric catalysts.

pure *S* product, and the *R* catalyst affords the *R* product in 100% ee (eqs 1 and 2).



When the asymmetric reaction is performed with a partially resolved chiral catalyst, stereoisomeric catalytic cycles compete in the same reaction system (Figure 1). In most asymmetric catalysis, the two enantiomeric catalyst systems are independent, and the reaction is first order with respect to the catalyst. Therefore, the initial reaction rate,  $v_0$ , is dependent on the catalyst concentration but is unaffected by the ratio of the catalyst enantiomers, whereas the enantioselectivity of the reaction varies linearly from *S* 100% to *R* 100% as a function of the ratio of the *S* and *R* catalyst. However, this is no longer valid when the catalyst enantiomers interact in the reaction system. In general, a chiral catalyst may interact with itself, the enantiomer, diastereomer, or even totally unrelated molecules, resulting in a substantial deviation from this standard situation. The following systematic studies will illustrate the significance of the self and nonself recognition of asymmetric catalysts.

### Reaction System

In order to study this subject at the molecular level, we selected as the standard catalytic system the reaction of

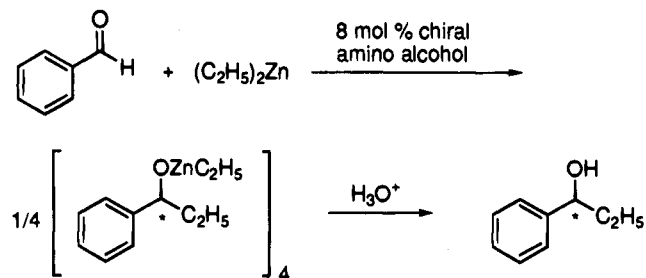


**Figure 2.** Enantioselective addition of diethylzinc to benzaldehyde promoted by an amino alcohol.

diethylzinc and benzaldehyde in the presence of an amino alcohol,<sup>9,16</sup> as shown in Figure 2.<sup>7-9,17</sup> The enantioselectivity and reactivity were examined in toluene at 0 °C. Although the previous investigation<sup>7-9</sup> found that diethyl- and dimethylzinc behave in a similar manner, we used diethylzinc for better reproducibility. The molecular weight measurements by cryoscopy were also done with the ethylzinc compounds which possess a higher solubility. Methylzinc complexes were used for structural analysis by X-ray crystallography and <sup>1</sup>H NMR because of their high crystallinity and low structural fluxionality. The ethyl analogues often displayed broad NMR signals, even at low temperatures, which are difficult to analyze. Chiral and achiral compounds **1** and **2**<sup>18,19</sup> were used as amino alcohol promoters (Figure 3). In the bicyclic compounds **1**, *R* and *S* refer to the configuration of the C(2) stereogenic position, X denotes the exo geometry of the C(3) dimethylamino group with respect to the bicyclo[2.2.1]heptane skeleton, while N denotes the endo stereochemistry.

### Interaction of Enantiomeric Catalysts

We reinvestigated enantioselective alkylation<sup>7-9</sup> using the standard conditions. As noted earlier, the reaction of diethylzinc (420 mM) and benzaldehyde (420 mM) at 0 °C in toluene in the presence of partially resolved [(*S*)-X]-**1** (34 mM) displays unique nonlinear effects. Figure 4 shows the rate and enantioselectivity as a function of the ratio of [(*S*)-X]- and [(*R*)-X]-**1**. Enantiomeric purity of the amino alcohol as well as reaction conditions appeared to strongly affect the reaction rate. Under the standard conditions, the reaction with racemic **1** proceeded 13 times slower than that with the enantiomerically pure *S* or *R* catalyst. In addition, the enantioselectivity deviated significantly from the anticipated values for the independent behavior of the enantiomerically pure catalysts. The ee values of the alcoholic product ranging from *S* 98% to *R* 98% were much higher than those of the amino alcohol **1**. The racemate was obtained only when **1** was racemic.

The reaction of benzaldehyde and diethylzinc is catalyzed by the ethylzinc aminoalkoxide **3** (R = C<sub>2</sub>H<sub>5</sub>) formed from diethylzinc and [(*S*)-X]- or [(*R*)-X]-**1** (Figure 5), according to a preliminary kinetic study.<sup>7-9</sup> However, under the above reaction conditions, the catalytic tricoordinate Zn species tends to dimerize in a reversible manner to form the dinuclear complex **4**. The nonlinearity of the reactivity and stereoselectivity are

(16) Soai, K.; Niwa, S. *Chem. Rev.* **1992**, *92*, 833.

(17) (a) Kitamura, M.; Suga, S.; Kawai, K.; Noyori, R. *J. Am. Chem. Soc.* **1986**, *108*, 6071. (b) Noyori, R.; Suga, S.; Kawai, K.; Okada, S.; Kitamura, M.; Oguni, N.; Hayashi, M.; Kaneko, T.; Matsuda, Y. *J. Organomet. Chem.* **1990**, *19*, 382.

(18) (a) Beckett, A. H.; Lan, N. T.; McDonough, G. R. *Tetrahedron* **1969**, *25*, 5689. (b) Beckett, A. H.; Lan, N. T.; McDonough, G. R. *Tetrahedron* **1969**, *25*, 5693. (c) Chittenden, R. A.; Cooper, G. H. *J. Chem. Soc. C* **1970**, 49. (d) Daniel, A.; Pavia, A. A. *Bull. Soc. Chim. Fr.* **1971**, 1060. (e) Reetz, M. T.; Zierke, T. *Chem. Ind.* **1988**, *17*, 663.

(19) Leonard, N. J.; Durand, D. A.; Uchimaru, F. *J. Org. Chem.* **1967**, *32*, 3607.

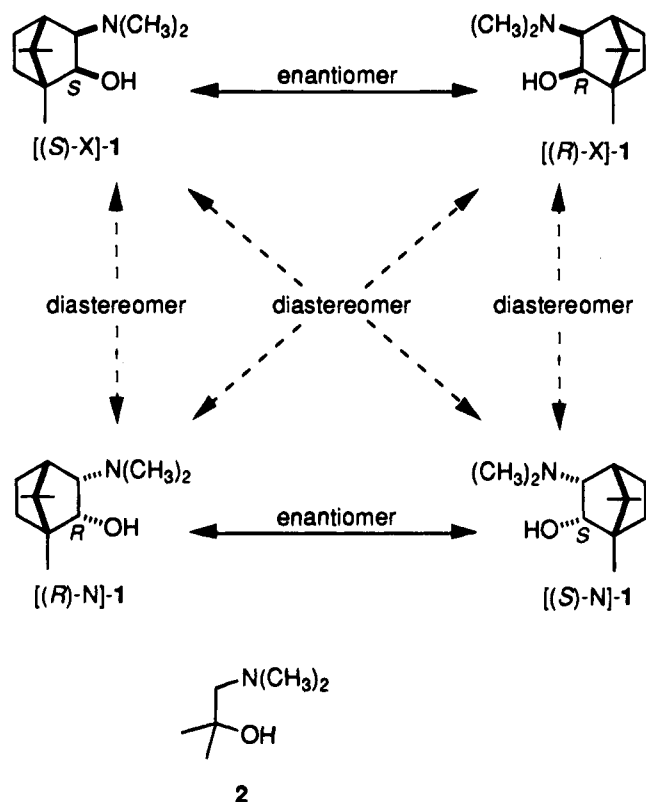


**Figure 3.** Chiral and achiral amino alcohols promoting the reaction of diethylzinc and benzaldehyde.

interpreted in terms of the relative stabilities of the diastereomers **4**. As illustrated in Figure 5, self recognition of the (*S*)-**X** or (*R*)-**X** monomer **3** forms the homochiral dimer (dinuclear complex formed from **3** with the same chirality), [(*S*)-**X**,(*S*)-**X**]-**4** or [(*R*)-**X**,(*R*)-**X**]-**4**, respectively, whereas their nonself recognition leads to the heterochiral dimer (dinuclear complex formed from the enantiomeric monomers) [(*S*)-**X**,(*R*)-**X**]-**4**. The molecular weight by cryoscopy<sup>7–9</sup> revealed that the heterochiral dimer is overwhelmingly more stable than the homochiral dimers. Molecular weight determination by vapor pressure osmometry<sup>20</sup> using the methylzinc complexes at varying concentrations has indicated that the dissociation constant of the homochiral dimer,  $K_{\text{homo}} \approx (3.0 \pm 1.0) \times 10^{-2}$ , is much larger than the value of the heterochiral dimer,  $K_{\text{hetero}} \approx 1 \times 10^{-5}$ , in toluene at 40 °C.<sup>20</sup> Consistent with the large difference in the *K* values, the Zn-methyl signal in the <sup>1</sup>H NMR spectrum of the heterochiral dimer is sharper than that of the homochiral dimer, the half-width being 1 vs 2 Hz (Figure 6, A-3 vs A-1 and A-2). Therefore, when partially resolved [(*S*)-**X**]-**1** is used as a chiral auxiliary, most of the minor (*R*)-**X** enantiomer is consumed by taking the same amount of the (*S*)-**X** isomer to form [(*S*)-**X**,(*R*)-**X**]-**4**, while the rest of the (*S*)-**X** isomer forms less stable [(*S*)-**X**,(*S*)-**X**]-**4** that promotes enantioselective alkylation via dissociation into the monomer. Such thermodynamic relationships of the diastereomers **4** are in accord with the marked chirality amplification of Figure 4. Furthermore, when partially resolved **1** is employed, the concentration of the monomer **3** is much less than when enantiomerically pure **1** is used owing to the high stability of [(*S*)-**X**,(*R*)-**X**]-**4** and consistent with the significant decrease of the reaction rate.

#### Interaction of Diastereomeric Catalysts

Alkylation experiments revealed that [(*R*)-**N**]-**1** as promoter is 2.6 times more reactive than its diastereomer (*S*)-**X**, giving

(20) Kitamura, M.; Suga, S.; Niwa, M.; Noyori, R.; Zhai, Z.-X.; Suga, H. *J. Phys. Chem.* **1994**, *98*, 12776.

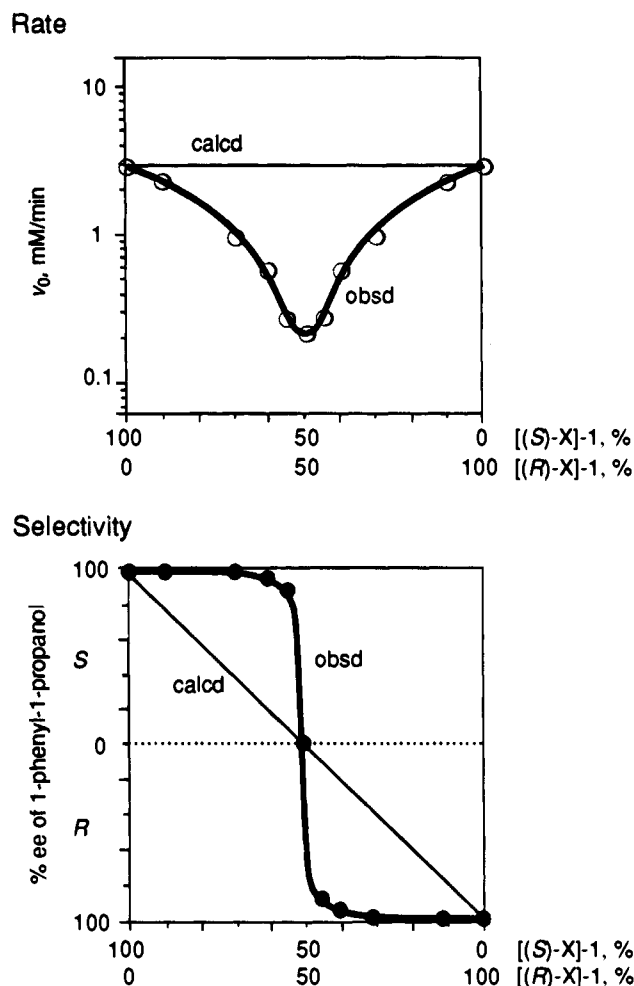


**Figure 4.** Nonlinear phenomena in the reaction of benzaldehyde (420 mM) and diethylzinc (420 mM) in the presence of enantiomeric amino alcohols, [(*S*)-**X**]-**1** and [(*R*)-**X**]-**1**, (34 mM) in toluene at 0 °C.

(*R*)-1-phenyl-1-propanol in 94% ee. Figure 7 illustrates the ee of the ethylation product obtained by use of a mixture of [(*S*)-**X**]- and [(*R*)-**N**]-**1**. The calculated lines, where the independence of the chiral catalysts is assumed, are not straight because of the diastereomeric, instead of enantiomeric, nature of the amino alcohols. Still the linearity is maintained when corrected for the difference in their reactivity. When the ethylation was conducted using mixtures of these diastereomeric auxiliaries, characteristic nonlinear relationships were seen again. The *S*-directing amino alcohol, [(*S*)-**X**]-**1**, and *R*-generating ancillary, [(*R*)-**N**]-**1**, even when mixed with a significant amount of the counterpart, exhibited an inherent sense of asymmetric induction. For instance, use of a 40:60 mixture of [(*S*)-**X**]-**1** and [(*R*)-**N**]-**1** afforded the *R* ethylation product in 94% ee. Only with the (*S*)-**X**/(*R*)-**N** ratio very close to unity was the enantioselectivity diminished. In addition, the alkylation with an equimolar mixture of [(*S*)-**X**]- and [(*R*)-**N**]-**1** was 17 times slower than with diastereomerically pure [(*S*)-**X**]-**1** and 45 times slower than with [(*R*)-**N**]-**1**.

The monomer–dimer equilibria of the catalyst system is given in Figure 8. The number average molecular weight of the Zn species was measured by cryoscopy using a benzene solution of the complexes prepared from a 2:1:1 mixture of diethylzinc, [(*S*)-**X**]-**1**, and [(*R*)-**N**]-**1**, or a 1:1 mixture of diethylzinc and [(*S*)-**X**]- or [(*R*)-**N**]-**1**. The observed values, which carry a 10% uncertainty, were 544–548 (42 mM solution), 550–572 (47 mM),<sup>8</sup> and 566–571 (38 mM), respectively, suggesting that all the stereoisomeric dinuclear complexes of type **4** retain mostly

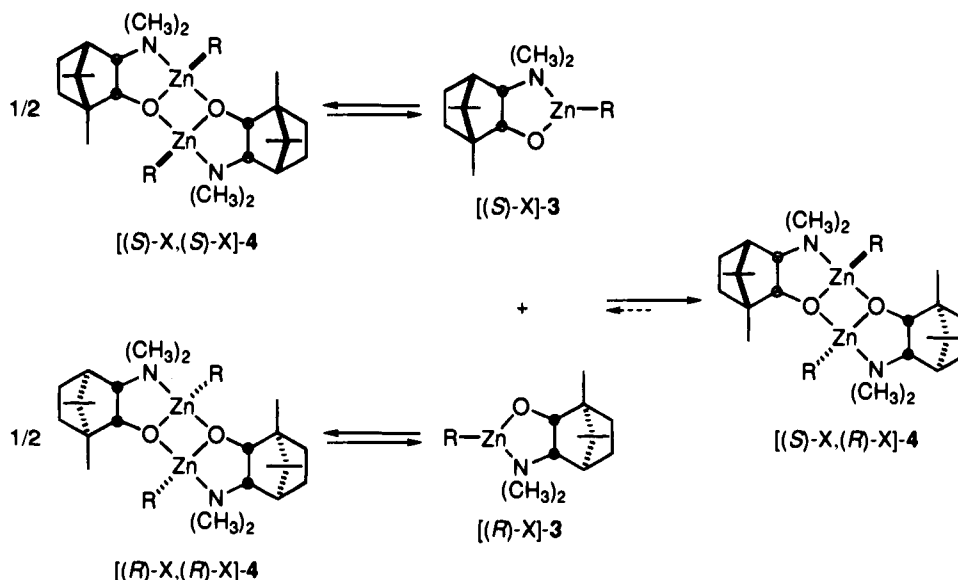


Figure 5. Self and nonself recognition of enantiomeric catalysts, [(S)-X]- and [(R)-X]-3.

the dinuclear form (calculated for **4** ( $R = C_2H_5$ ), 581.5) in a >40 mM hydrocarbon solution. These experimental values, however, were lower than the calculated values, suggesting some dissociation into their monomers.

The nonlinear effect of Figure 7 can be ascribed to a very strong nonself recognition of the Zn catalysts **3**. The (S)-X and (R)-N catalysts associate tightly to produce a stable dinuclear Zn complex, [(S)-X,(R)-N]-**4**. In fact the reaction of dimethylzinc and the amino alcohols [(S)-X]- and [(R)-N]-**1** (2:1:1 mole ratio) in toluene afforded selectively the crystalline mixed dimer [(S)-X,(R)-N]-**4** ( $R = CH_3$ ). Single crystal X-ray analysis indicates an *S,R* configuration at the tetrahedral Zn atoms (Figure 9A). The central 5/4/5 tricyclic structure indeed has a sterically uncongested anti geometry as in [(S)-X,(R)-X]-**4**.<sup>8</sup> The self-association of the catalyst **3** leading to [(S)-X,(S)-X]- or [(R)-N,(R)-N]-**4**, on the other hand, is thermodynamically less favored. Consistent with the *S,S* configuration at the Zn atoms in [(S)-X,(S)-X]-**4** and [(R)-N,(R)-N]-**4** ( $R = CH_3$ ) probably possesses a highly crowded *syn*-5/4/5 tricyclic system owing to the presence of the bornyl skeleton where the Zn stereogenic centers have *R,R* geometry.

The <sup>1</sup>H NMR spectrum of [(R)-N,(R)-N]-**4** ( $R = CH_3$ ) (2 mM toluene-*d*<sub>8</sub> solution, 25 °C) showed only a single set of Zn-methyl, N-methyl, and C(2)-H signals at  $\delta -0.07$ , 2.23, and 4.27, respectively, which was consistent with the proposed *C*<sub>2</sub>-symmetrical structure. When the concentration of the Zn complex was increased to 10 mM, a small, new set of signals appeared (ca. 5–10%: including a singlet at  $\delta$  0.10 due to Zn-CH<sub>3</sub>), which could be assigned to a tetramer of [(R)-N]-**3**<sup>21</sup> with a Zn<sub>4</sub>O<sub>4</sub> eight-membered ring.<sup>22</sup> Notably, an equimolar mixture of [(S)-X,(S)-X]-**4** and [(R)-N,(R)-N]-**4** (10 mM toluene-*d*<sub>8</sub> solution, 25 °C) gave the same spectrum as that of [(S)-X,(R)-N]-**4**. The latter unsymmetrical compound displayed two singlets due to the diastereotopic Zn-methyl groups ( $\delta -0.33$  and  $-0.16$ ), four singlets due to the N-methyl groups, and one intense and four ordinary singlets due to the six different C-methyl groups. Signals from the self dimers, [(S)-X,(S)-X]-**4** and [(R)-N,(R)-N]-**4**, were not observed (Figure 6, B-3). When the self dimer was present in excess, the self and nonself

dimers showed separate signal sets. The lack of coalescence even at 100 °C indicates the structural rigidity of the nonself dimer. This was also supported by the Zn-CH<sub>3</sub> signals which were sharper (half-width 1 Hz) than those of the self dimers (2 Hz) (Figure 6, B-3 vs B-1 and B-2). The <sup>13</sup>C NMR spectrum gave 26 separate signals further confirming the hetero dinuclear structure. These facts clearly indicate the thermodynamic preference of the nonself association of [(S)-X]-**3** and [(R)-N]-**3** in the solution phase.

The stereoisomers of **4** thus have distinctly different properties (Figure 8). In the reaction with an (S)-X/(R)-N mixed amino alcohol system, the nonself associate, [(S)-X,(R)-N]-**4**, barely acts as a catalyst precursor owing to its high stability. Instead the reactive monomer **3** is generated preferentially by cleavage of the less stable self dimer, [(S)-X,(S)-X]- or [(R)-N,(R)-N]-**4**, present in excess in the reaction system. As a consequence, a high degree of enantioselection is obtained even in the presence of a large amount of the diastereomeric catalyst. However, the concentration of the self dimers is much lower than with the diastereomerically pure amino alcohol, resulting in a slower reaction. Consistent with this view, the lowest rate was obtained with a 50:50 mixture of [(S)-X]-**1** and [(R)-N]-**1** as promoter.

Yet another effect has been found in the asymmetric ethylation with a combined system of [(S)-X]- and [(S)-N]-**1** (Figure 3). These auxiliaries, though the functionalities have contrasting *exo* and *endo* configurations with respect to the bicycloheptane framework, are both *S*-directing, because the absolute configurations of C(2) are both *S*. The catalysis with enantiomerically pure [(S)-N]-**1** proceeds 2.6 times faster than with pure [(S)-X]-**1** and with a slightly lower (3–4%) enantioselectivity. As seen in Figure 10, the velocity of the ethylation obtained with the mixed stereoisomers is lower than the calculated value but the deviation is rather small. The observed selectivity profile fits well with the calculated values.

Cryoscopic measurement of the number average molecular weight of the Zn complexes revealed the existence of the equilibrating system shown in Figure 11. Thus a 46 mM benzene solution of the compound formed from a 2:1:1 mixture of diethylzinc, [(S)-X]-**1**, and [(S)-N]-**1** afforded the value of 510–549 (calcd for **4** ( $R = C_2H_5$ ), 581.5), in accordance with the equilibria between major dinuclear complexes **4** and minor monomers **3**. This equilibrating system, unlike those in Figures

(21) (a) van der Steen, F. H.; Boersma, J.; Spek, A. L.; van Koten, G. *Organometallics* **1991**, *10*, 2467. (b) van der Schaaf, P. A.; Wissing, E.; Boersma, J.; Smeets, W. J. J.; Spek, A. L.; van Koten, G. *Organometallics* **1993**, *12*, 3624.

(22) These signals are absent in the spectrum taken at 80 °C.

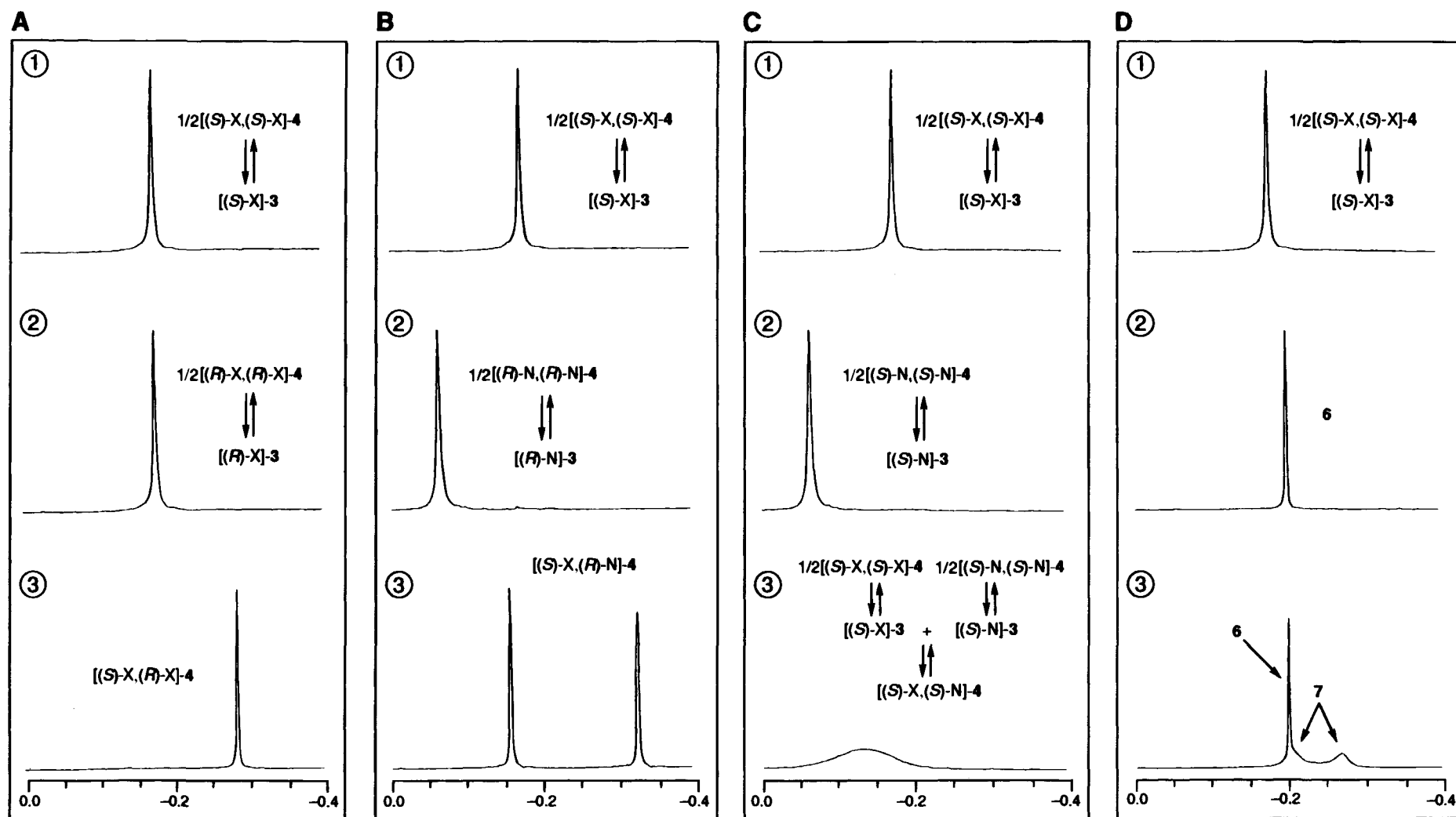
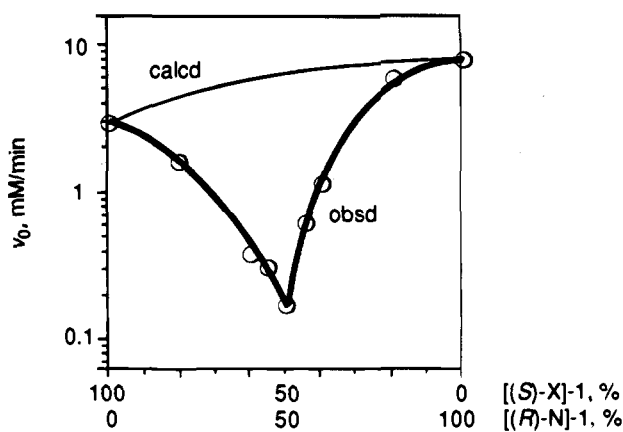


**Figure 6.** Zn-CH<sub>3</sub> signals in the <sup>1</sup>H NMR spectra taken in toluene-*d*<sub>8</sub> (10–20 mM) at 25 °C. Chemical shift is given in δ values. A-1: (CH<sub>3</sub>)<sub>2</sub>Zn and [(*S*)-X]-1 (1:1). A-2: (CH<sub>3</sub>)<sub>2</sub>Zn and [(*R*)-X]-1 (1:1). A-3: (CH<sub>3</sub>)<sub>2</sub>Zn, [(*S*)-X]-1, and [(*R*)-X]-1 (2:1:1) giving [(*S*)-X,(*R*)-X]-4. B-1: (CH<sub>3</sub>)<sub>2</sub>Zn and [(*S*)-X]-1 (1:1). B-2: (CH<sub>3</sub>)<sub>2</sub>Zn and [(*R*)-N]-1 (1:1). B-3: (CH<sub>3</sub>)<sub>2</sub>Zn, [(*S*)-X]-1, and [(*R*)-N]-1 (2:1:1) giving [(*S*)-X,(*R*)-N]-4. C-1: (CH<sub>3</sub>)<sub>2</sub>Zn and [(*S*)-X]-1 (1:1). C-2: (CH<sub>3</sub>)<sub>2</sub>Zn and [(*S*)-N]-1 (1:1). C-3: (CH<sub>3</sub>)<sub>2</sub>Zn, [(*S*)-X]-1, and [(*S*)-N]-1 (2:1:1). D-1: (CH<sub>3</sub>)<sub>2</sub>Zn and [(*S*)-X]-1 (1:1). D-2: (CH<sub>3</sub>)<sub>2</sub>Zn and **2** (1:1) giving **6**. D-3: (CH<sub>3</sub>)<sub>2</sub>Zn, [(*S*)-X]-1, and **2** (3:1:2) giving **6** and **7** (1:2).

## Rate



## Selectivity

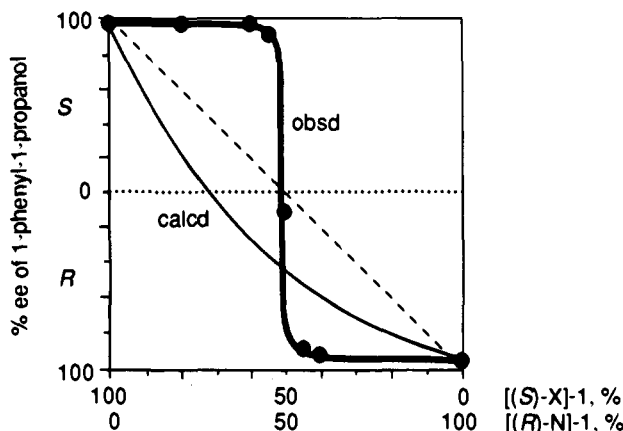


**Figure 7.** Nonlinear phenomena in the reaction of benzaldehyde (420 mM) and diethylzinc (420 mM) in the presence of diastereomeric amino alcohols, [(*S*)-X]-1 and [(*R*)-N]-1, (34 mM) in toluene at 0 °C. The broken line indicates the values when the reactivity difference between the diastereomeric catalysts is not considered.

5 and 8, is characterized by the easy dissociation of the nonself associate [(*S*)-X,(*S*)-N]-4 as demonstrated below.

The properties of the self dimers [(*S*)-X,(*S*)-X]-4 and [(*S*)-N,(*S*)-N]-4 (identical with the (*R*)-N,(*R*)-N enantiomer) are already known. Although three diastereomers are conceivable for the adduct of [(*S*)-X]-3 and [(*S*)-N]-3, model inspection reveals that the syn-5/4/5-tricyclic structure [(*S*)-X,(*S*)-N]-4 is a sole possibility, owing to the presence of the bornane skeleton, and the Zn centers have the *S,S* configuration.<sup>23</sup> In toluene solution, the mixed dimer, [(*S*)-X,(*S*)-N]-4 (*R* = CH<sub>3</sub>), readily dissociates into monomeric [(*S*)-X]- and [(*S*)-N]-3, which in turn undergo either self or nonself association. Consistent with this facile exchange, the <sup>1</sup>H NMR spectrum (10 mM toluene-*d*<sub>8</sub> solution, 25 °C) gave very broad signals as exemplified by the Zn-CH<sub>3</sub> signal at  $\delta$  -0.14 in Figure 6, C-3.

In contrast to the above described cases, the observed rate and selectivity as shown in Figure 10 display only slight deviations from the calculated profiles where the independence of the two diastereomeric catalytic cycles involving the (*S*)-X- and (*S*)-N catalysts is assumed. Mixed use of the diastereomeric amino alcohols, [(*S*)-X]-1 and [(*S*)-N]-1, did not cause deceleration to any great extent, while the enantioselectivity remained

(23) A single crystal obtained from a 2:1:1 mixture of dimethylzinc, [(*S*)-X]-1, and [(*S*)-N]-1 in toluene was found to consist of [(*S*)-X,(*S*)-N]-4 and [(*S*)-X,(*S*)-X]-4 in a 2:1 ratio. The X-ray data of the disordered single crystal with *R* value of 0.059 revealed that [(*S*)-X,(*S*)-N]-4 has the syn 5/4/5 geometry.

consistently high. The tricoordinate Zn complexes [(*S*)-X]- and [(*S*)-N]-3 (Figure 11) acted as true catalysts and equilibrated with the dinuclear compounds, while the diastereomeric assemblage, either self or nonself, provided little thermodynamic advantage. Because of the common syn geometry with respect to the central 5/4/5-tricyclic ring system, the three dinuclear Zn complexes [(*S*)-X,(*S*)-X]-, [(*S*)-N,(*S*)-N]-, and [(*S*)-X,(*S*)-N]-4, have comparable and lower stabilities than the anti complexes such as [(*S*)-X,(*R*)-X]-4 and [(*S*)-X,(*R*)-N]-4. Since such dinuclear species dissociate into the catalytic monomers with approximately even distribution, the total concentration of the catalytic species 3 is reduced less than when using the stereochemically pure (*S*)-X- or (*S*)-N compound. Because both stereoisomeric catalysts efficiently direct the formation of the *S* product, the enantioselectivity is unaffected by the isomer ratio. Overall, this system is relatively linear with respect to both rate and stereoselectivity.

### Interaction between a Chiral Catalyst and an Achiral Catalyst

The coexistence of an achiral component also brings about nonlinear effects. When the achiral auxiliary, 2-(dimethylamino)-1,1-dimethylethanol (**2**) was added to the ethylation of benzaldehyde catalyzed by [(*S*)-X]-1, the stereoselectivities were uniquely affected (Figure 3). It was found that the ethylation promoted by the simple alcohol **2** under standard conditions proceeded 34 times slower than with [(*S*)-X]-1. When the reaction was carried out with a mixture of [(*S*)-X]-1 and **2**, the rate was notably suppressed as shown in Figure 12. The degree of the departure from the calculated line is significant with [(*S*)-X]-1/2 < 1. Since the inherent enantioselectivities given by [(*S*)-X]-1 and **2** are entirely different, *S* 98% ee vs racemic, the reaction results in substantial deviation from the expected stereoselectivities. When the chiral amino alcohol was used in excess, the *S* product was obtained in very high ee. The observed enantioselectivity was higher but very close to the calculated value when the difference in the reactivity of [(*S*)-X]-1 and **2** is considered. The reaction using a 60:40 mixture of the two amino alcohols gave the *S* ethylation product in 97% ee. On the other hand, the catalysis with the 20:80 mixture afforded the *S* product in 62% ee, which was considerably lower than the expected 88% ee. The reaction rate was also 2.4 times slower than the calculated one. The observed and calculated curves intersect when the chiral and achiral auxiliaries are used in equal amounts.

The equilibrium shown in Figure 13, which involves the three nonstereoisomeric dinuclear Zn complexes with markedly different stabilities, reasonably explains these results. The cryoscopic analysis of a 37 mM benzene solution of **6** (*R* = C<sub>2</sub>H<sub>5</sub>) formed from equimolar amounts of diethylzinc and **2** gave the dimeric molecular weight, 403–421 (calcd, 421.2). An 80 mM solution of a 1:1 mixture of **6** and [(*S*)-X,(*S*)-X]-4 showed the value of 491–497 (calcd for **7** or the average of **6** and [(*S*)-X,(*S*)-X]-4, 501.4), suggesting the formation of the major dinuclear Zn structures.

Although an anti-5/4/5 structure (meso) and the syn stereoisomers (*S,S* and *R,R* at Zn atoms) are possible for **6**, the latter is highly improbable because of the strong C-CH<sub>3</sub>/N-CH<sub>3</sub> nonbonded repulsion. The single crystal X-ray crystallographic analysis of the dimer **6** (*R* = CH<sub>3</sub>) (Figure 9B) indeed substantiated the anti geometry. Furthermore, the crystalline mixed dinuclear complex **7** (*R* = CH<sub>3</sub>) could also be obtained from a 2:1:1 molar mixture of dimethylzinc, [(*S*)-X]-1, and **2** in toluene. The X-ray analysis given in Figure 9C clarified the anti 5/4/5 geometry as well as the *S,R* absolute configuration at the Zn atoms.

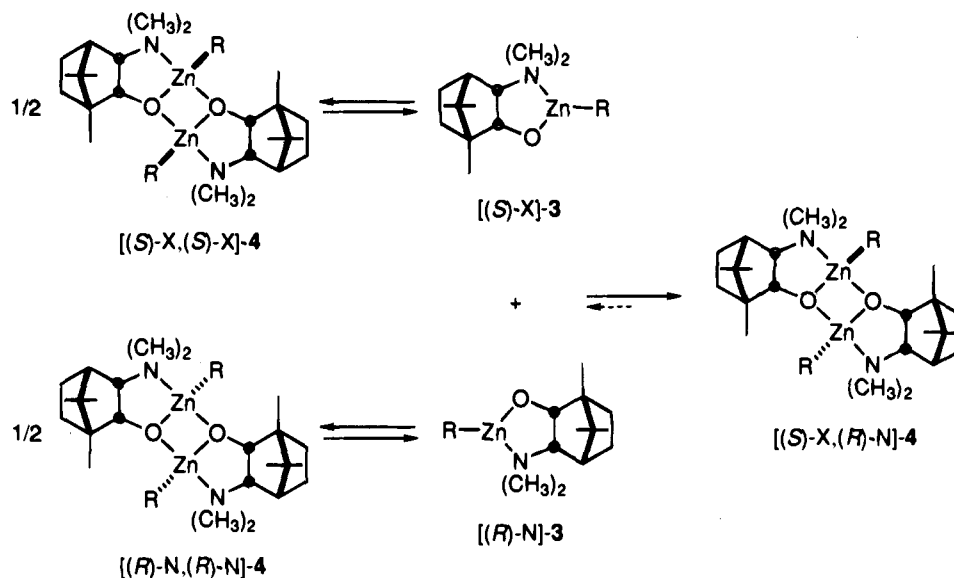


Figure 8. Self and nonself recognition of diastereomeric catalysts,  $[(S)\text{-X}]\text{-}$  and  $[(R)\text{-N}]\text{-3}$ .

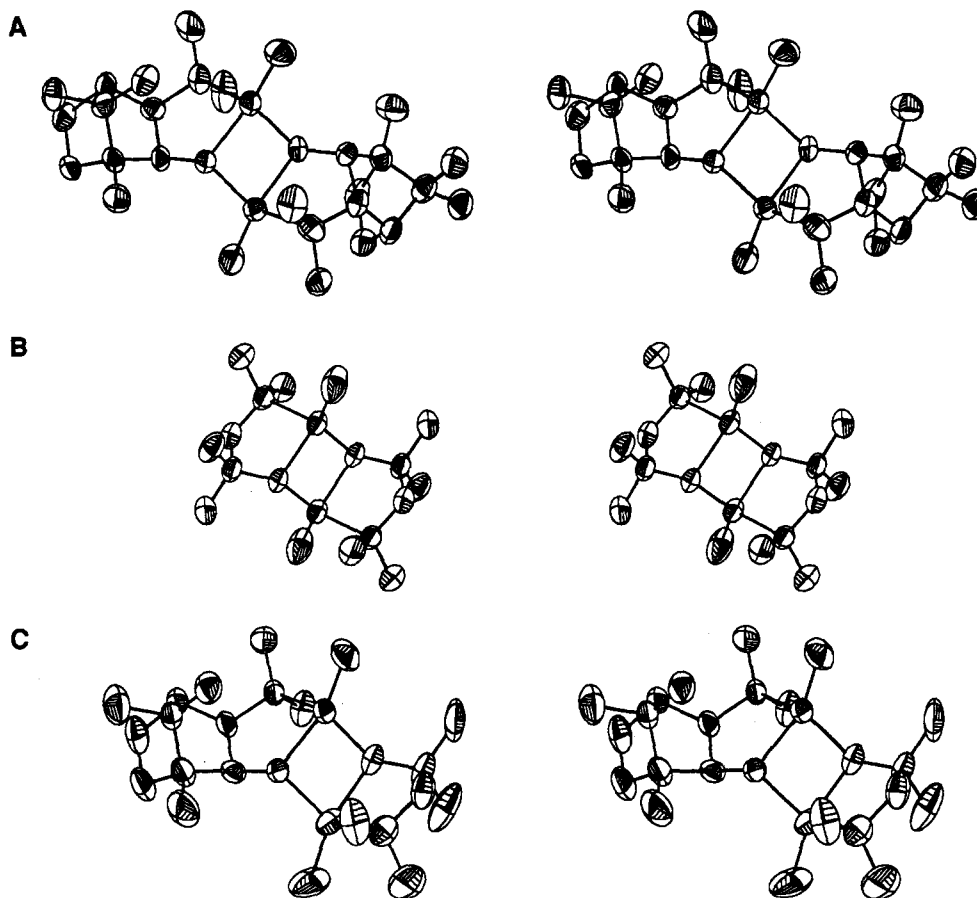
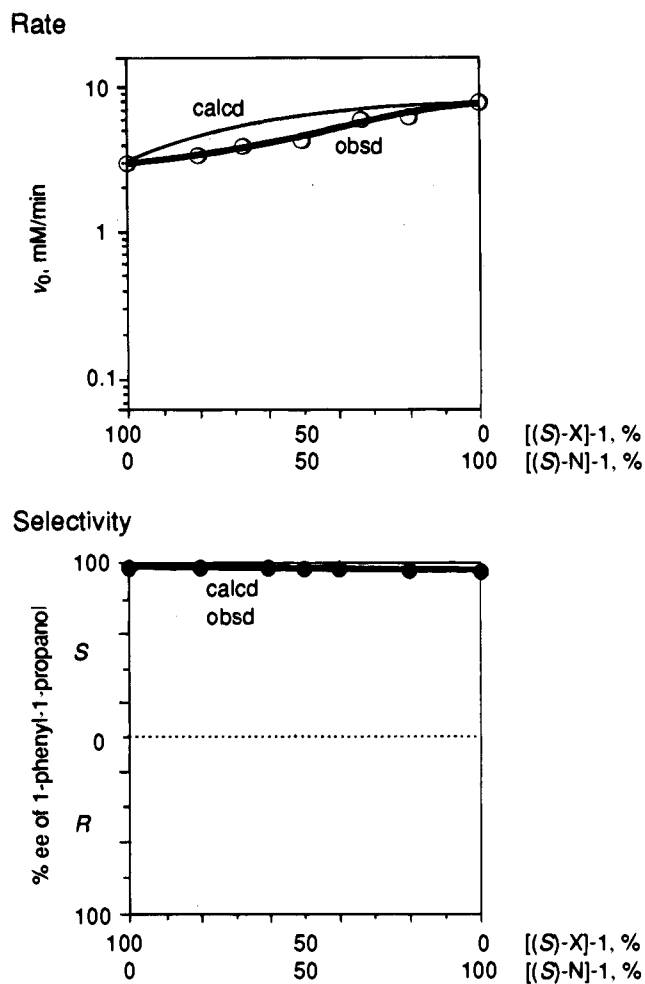


Figure 9. ORTEP stereoviews of the dinuclear methylzinc alkoxides: (A)  $[(S)\text{-X},(R)\text{-N}]\text{-4}$  ( $R = \text{CH}_3$ ), (B) **6** ( $R = \text{CH}_3$ ), (C) **7** ( $R = \text{CH}_3$ ).

The achiral compound **6** largely maintains the dimeric framework in toluene. Unlike the chiral dimer  $[(S)\text{-X},(S)\text{-X}]\text{-4}$  ( $R = \text{CH}_3$ ), which is in equilibrium with the monomer  $[(S)\text{-X}]\text{-3}$ , the achiral dimer **6** undergoes rapid intramolecular structural changes (ring flipping), while the dimeric structure is maintained. The  $^1\text{H}$  NMR spectrum at  $-60^\circ\text{C}$  of a 20 mM toluene- $d_8$  solution of the organozinc compound formed by mixing equimolar amounts of dimethylzinc and **2** indicated the equivalence of the two Zn-methyl groups and nonequivalence of the C- and N-methyl groups and the methylene protons as is consistent with the geometry of **6**. At room temperature,

however, the dissociation of the weak Zn–N bond in **6**<sup>24</sup> caused facile configurational inversion at the Zn and O atoms via the transient syn isomer, resulting in chemical shift equivalence of the otherwise nonequivalent protons. Thus the spectrum at  $25^\circ\text{C}$  showed sharp singlets due to the Zn-methyl, C-methyl,  $\text{CH}_2$ , and N-methyl protons at  $\delta -0.20$ , 1.44, 2.34, and 2.38, respectively. Notably, this time-averaging phenomenon is intramolecular in nature and not due to the dimer–monomer equilibration,  $\mathbf{6} \rightleftharpoons \mathbf{5}$ . The Zn-methyl signals were kept sharp in a range of  $25\text{--}100^\circ\text{C}$  (Figure 6, D-2).

(24) Haaland, A. *Angew. Chem., Int. Ed. Engl.* 1989, 28, 992.



**Figure 10.** Rate and enantioselectivity of the reaction of benzaldehyde (420 mM) and diethylzinc (420 mM) in the presence of diastereomeric amino alcohols, [(S)-X]-1 and [(S)-N]-1, (34 mM) in toluene at 0 °C.

When a half equivalent of [(S)-X,(S)-X]-4 ( $R = \text{CH}_3$ ) was added to **6**, a new spectrum was obtained which was assignable to a 1:2, independent mixture of **6** and the mixed complex **7** (Figure 6, D-3). The dinuclear complex **7**, though dissociable, had relatively high stability as proved by the  $^1\text{H}$  NMR behavior of the methyl complexes; it gave two broad Zn-methyl signals at  $\delta -0.27$  and  $-0.20$  with equal intensities. In going from **5** to **7**, the originally enantiotopic C- and N-methyls became diastereotopic giving two separate signals at  $\delta 1.40$  and  $1.48$  and  $2.31$  and  $2.51$ , respectively, whereas the methylene proton signals had an AB pattern at  $\delta 2.22$  and  $2.59$  with  $J = 13.2$  Hz. The broadness of the Zn-CH<sub>3</sub> signals (half-width 7 Hz), indicates that this mixed dinuclear complex might cleave into [(S)-X]-3 and **5** in toluene but enjoys considerable stability. Consistent with this, a 3:2:1 mixture of dimethylzinc, [(S)-X]-1, and **2** afforded the separate NMR signals of **7** and [(S)-X,(S)-X]-4 equilibrating with [(S)-X]-3 in a 2:1 to 3:2 ratio at the expense of the achiral dimer **6**. At 100 °C, however, the signals are completely averaged, giving, for instance, a sharp Zn-CH<sub>3</sub> singlet. The mixed compound **7** appears not as rigid as [(S)-X,(R)-X]-4 and [(S)-X,(R)-N]-4, but the dissociation constant is several hundred times smaller than that of [(S)-X,(S)-X]-4, [(S)-N,(S)-N]-4, or [(S)-X,(S)-N]-4. Thus the stability of the dinuclear structure appears to decrease in the order of  $\mathbf{6} > \mathbf{7} \gg [(S)-X,(S)-X]-4$ .

These observations are fully in accord with the nonlinear effects shown in Figure 12. The high stability of the self dimer **6** explains the low rate of the reaction with pure **2**. When the

chiral auxiliary [(S)-X]-1 is employed in excess to the achiral **2**, the minor achiral catalyst stays as the stable dimer **6** or forms the stable mixed complex **7**, while the remaining [(S)-X]-3 equilibrates with [(S)-X,(S)-X]-4 and acts as a major catalyst. The higher stability of the homodimer **6** with respect to the heterodimer **7** causes rather weak nonlinear effects in the region of  $[(S)-X]-1/2 > 1$ . If **7** were more stable than **6**, a larger departure would be observed owing to the decrease of the net concentration of [(S)-X]-3. On the other hand, as the amount of **2** increases, considerable nonlinear effects are seen in both reaction rate and stereoselectivity. When the achiral auxiliary is used in large excess, the minor chiral component [(S)-X]-3 is mostly trapped by **5** to form the mixed complex and becomes inert in the catalytic system. The extent of the self-recognition of the achiral catalyst **5** is higher than that of any chiral catalyst tested in this work. Thus the self/nonself-recognition of the chiral and achiral zinc alkoxides has proved to affect the rate and stereoselectivity of the catalysis.

It should be added that the addition of non-amino alcohols such as methanol, *tert*-butyl alcohol, and (*S*)- or (*R*)-1-phenyl-1-propanol affects neither the initial reaction rate nor the enantioselectivity of the ethylation of benzaldehyde promoted by [(S)-X]-1. The ethylzinc alkoxides derived from these alcohols form the stable self-aggregates, mostly tetramers,<sup>25</sup> and exist as independent entities in the catalytic system.

## Conclusion

This present systematic investigation of the four different types of amino alcohol combinations clearly shows that the rate and stereoselectivity of certain catalytic reactions are highly affected by the chemical and stereochemical (in relative and absolute sense) purity of the catalysts and is controlled by the self- or nonself-recognition of the catalysts. The relative significance strongly affects the overall profile of the asymmetric catalysis, which is highly dependent on the nature of the catalyst components. Although this effect has not seriously been appreciated, care should be taken in designing and performing catalytic reactions in general. Its clever use<sup>26</sup> may lead to a practical, significant asymmetric catalysis.

## Experimental Section

**General Methods.**  $^1\text{H}$ - and  $^{13}\text{C}$ -NMR spectra were measured in chloroform-*d* containing 0.03% tetramethylsilane as an internal standard or toluene-*d*<sub>8</sub> on a JEOL JNM-GX270, JNM-GSX270, or JNM- $\alpha$ 400 spectrometer. Chemical shifts are reported in ppm ( $\delta$ ) downfield from the tetramethylsilane, and the coupling constants ( $J$ ) were expressed in Hz. When measuring with toluene-*d*<sub>8</sub>, the methyl proton signal at  $\delta 2.31$  ( $^1\text{H}$  NMR) or 20.4 ( $^{13}\text{C}$  NMR) was used as a standard. The coupling patterns of singlet, doublet, triplet, quartet, multiplet, and broad signals were abbreviated to s, d, t, q, m, and br, respectively. Optical rotation was measured on a JASCO DIP-181 digital polarimeter with a 5 mm  $\times$  10 cm cell. X-ray crystallographic analysis was conducted on a Rigaku automated four-circle diffractometer AFC-5R or AFC-7R. Melting points were determined on a YANAKO micro melting point apparatus and were uncorrected. Gas-liquid phase chromatog-

(25) (a) Coates, G. E.; Ridley, D. *J. Chem. Soc.* **1965**, 1870. (b) Coates, G. E.; Ridley, D. *J. Chem. Soc., A* **1966**, 1064. (c) Noltes, J. G.; Boersma, J. *J. Organomet. Chem.* **1968**, *12*, 425. (d) Shearer, H. M. M.; Spencer, C. B. *Acta Crystallogr.* **1980**, *B36*, 2046. (e) Olmstead, M. M.; Power, P. P.; Shoner, S. C. *J. Am. Chem. Soc.* **1991**, *113*, 3379. (f) Herrmann, W. A.; Bogdanović, S.; Behm, J.; Denk, M. *J. Organomet. Chem.* **1992**, *430*, C33.

(26) (a) Maruoka, K.; Yamamoto, H. *J. Am. Chem. Soc.* **1989**, *111*, 789. (b) Faller, J. W.; Parr, J. *J. Am. Chem. Soc.* **1993**, *115*, 804. (c) Faller, J. W.; Tokunaga, M. *Tetrahedron Lett.* **1993**, *34*, 7359. (d) Faller, J. W.; Mazziere, M. R.; Nguyen, J. T.; Parr, J.; Tokunaga, M. *Pure Appl. Chem.* **1994**, *66*, 1463.

(27) Liu, J. H.; Kondo, K.; Takemoto, K. *Angew. Makromol. Chem.* **1984**, *121*, 106.



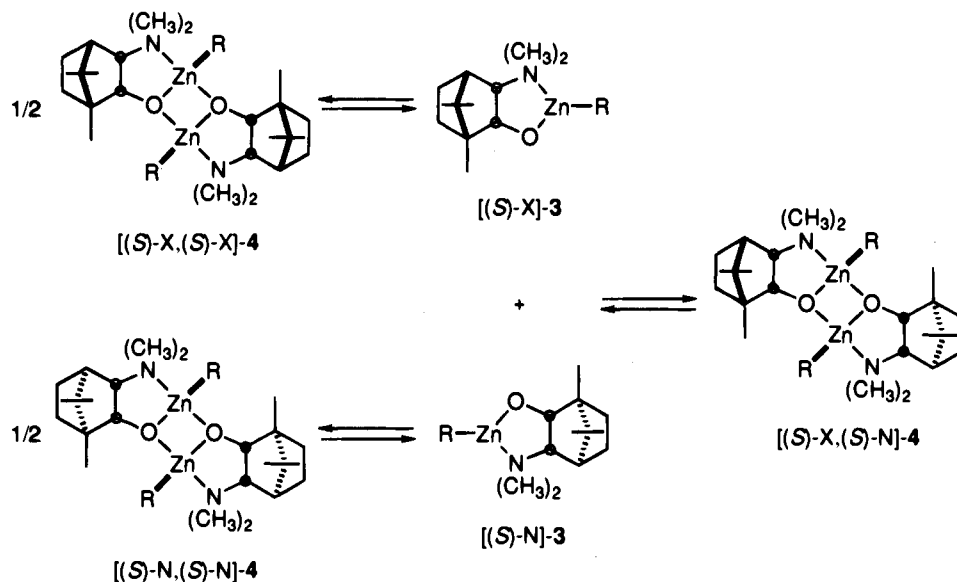
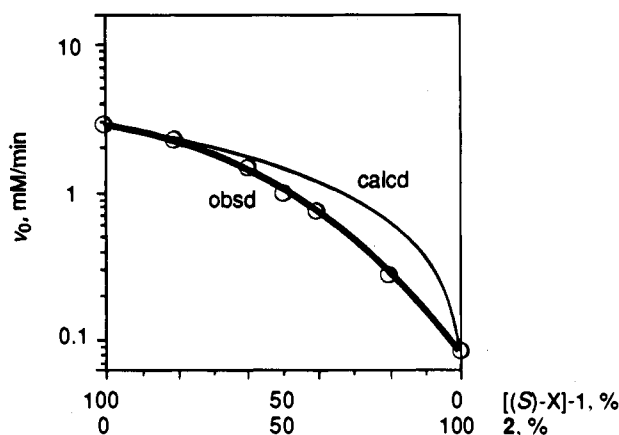


**Figure 11.** Self and nonself recognition of diastereomeric catalysts, [(S)-X]- and [(S)-N]-3.

### Rate



### Selectivity

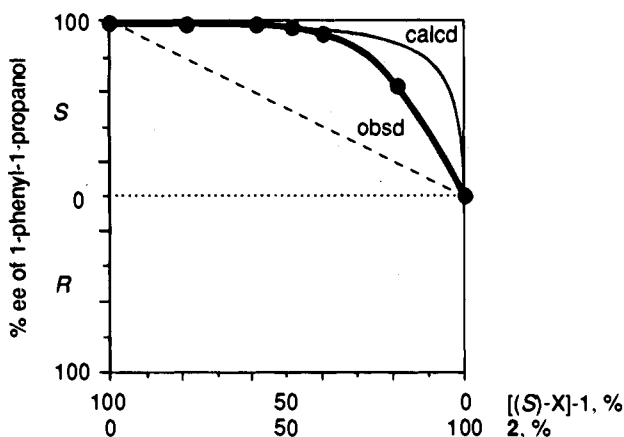


**Figure 12.** Rate and enantioselectivity of the reaction of benzaldehyde (420 mM) and diethylzinc (420 mM) in the presence of chiral and achiral amino alcohols, [(S)-X]-1 and 2 (34 mM), in toluene at 0 °C. The broken line indicates the values when the reactivity difference between [(S)-X]-1 and 2 is not considered.

raphy analyses by FID detection were performed on a Shimadzu GC-14A or GC-15A instrument. Liquid chromatographic analyses were conducted on a Shimadzu LC-6A instrument equipped with a RHEODYNE 7125 injector and a Shimadzu SPD-6A UV detector. Chromatography was done on a column of silica gel (Merck 7734 and 9385).

All alkylation experiments were performed under an argon atmosphere using standard Schlenk techniques.

**Materials.** Toluene and toluene- $d_8$  for the alkylation experiments, molecular weight measurements, and kinetics studies were distilled from a Na-K alloy and stored in a Schlenk tube. Dimethylzinc purchased from Toyo Stauffer Chemical Co., Lot No. DMZ 812, was purified by vacuum distillation. Diethylzinc, available from Toyo Stauffer Chemical Co., Lot No. DEZ 948, was used without purification. All stock solutions were kept in Schlenk tubes equipped with a Young's tap. Benzaldehyde was purified by distillation from 4Å molecular sieves and kept in a Schlenk tube. The crude (2*S*)- and (2*R*)-3-*exo*-(dimethylamino)isoborneol ([*(S)*-X]-1 and [*(R)*-X]-1) were prepared by the known method.<sup>18</sup> The optically and chemically pure [(S)-X]- and [(R)-X]-1 were obtained according to the reported method.<sup>17b</sup> The enantiomeric purities of these compounds were confirmed by HPLC analysis of the *N*-3,5-dinitrophenylcarbamates (column, Sumitomo Chemical Co. SUMIPAX OA-4000; eluent, 99.5:0.5 hexane-ethanol mixture; flow rate, 1.0 mL/min; detection, 254-nm light;  $t_R$ , 17.4 min (carbamate from [(S)-X]-1) and 22.5 min (carbamate from [(R)-X]-1). The achiral amino alcohol 2 was prepared by the known procedure.<sup>19</sup>

**Purification of [(S)-N]-1 and [(R)-N]-1.** The crude (2*R*)- and (2*S*)-3-*endo*-(dimethylamino)borneol ([*(R)*-N]-1 and [*(S)*-N]-1) were prepared through 3-*endo*-aminobornane-2-one, 3-*endo*-aminoborneol from (1*R*)-camphor ( $[\alpha]_D^{20} +45.2$  (*c* 9.7, ethanol)) and (1*S*)-camphor ( $[\alpha]_D^{20} -42.9$  (*c* 10.0, ethanol)) according to the reported method.<sup>18</sup> The crude [(R)-N]-1 (10.6 g, 0.0537 mol) and ethanol (39 mL) were placed in a 1-L round-bottomed flask, and an equimolar amount of (1*R*)-(-)-10-camphorsulfonic acid (12.5 g, 0.0537 mol) was added. The resulting solution was warmed to reflux temperature, and ethyl acetate (460 mL) and hexane (81 mL) were introduced at the same temperature. The whole system was kept at 25 °C for 12 h to produce a white solid, which was recrystallized an additional two times to give a colorless crystal (7.33 g,  $[\alpha]_D^{18} +1.86$  (*c* 3.43, ethanol)). The pure ammonium sulfate was partitioned between dichloromethane (100 mL) and 1 M aqueous NaOH (70 mL). The aqueous layer was extracted two times with dichloromethane (100 mL). The combined organic layers were washed successively with saturated NaHCO<sub>3</sub> solution (200 mL), water (200 mL), and saturated NaCl solution (200 mL). Drying over anhydrous Na<sub>2</sub>SO<sub>4</sub>, filtration, and evaporation of the solvent afforded an oil (2.51 g). Distillation from molecular sieves 4A at 157–165 °C and 21 mmHg using a Kugelrohr apparatus gave [(R)-N]-1 (2.29 g, 22% yield): <sup>1</sup>H NMR (270 MHz, CDCl<sub>3</sub>)  $\delta$  0.87 (s, 3, CH<sub>3</sub>), 0.89 (s, 6, 2 CH<sub>3</sub>), 1.12–1.23 (m, 1, CHH), 1.42–1.50 (m, 2, CH<sub>2</sub>), 1.67 (dd, 1, *J* = 4.0, 4.0 Hz, CH), 1.78–1.88 (m, 1, CHH), 2.21 (s, 6, N(CH<sub>3</sub>)<sub>2</sub>), 2.40 (ddd, 1, *J* = 1.1, 4.0, 8.7 Hz, NCH), 3.41 (br s, 1, OH), 3.64 (d, 1, *J* = 8.7 Hz, CHOH); <sup>13</sup>C NMR (100 MHz, CDCl<sub>3</sub>)  $\delta$  14.5, 18.9, 19.0, 20.0, 26.4, 45.1, 45.1, 45.3, 48.5, 50.3, 66.1, 74.0;  $[\alpha]_D^{20} +37.8$  (*c* 1.56, ethanol) [lit.<sup>27</sup>  $[\alpha]_D^{20} +24.2$  (*c* 1.56, benzene)]. The <sup>1</sup>H NMR

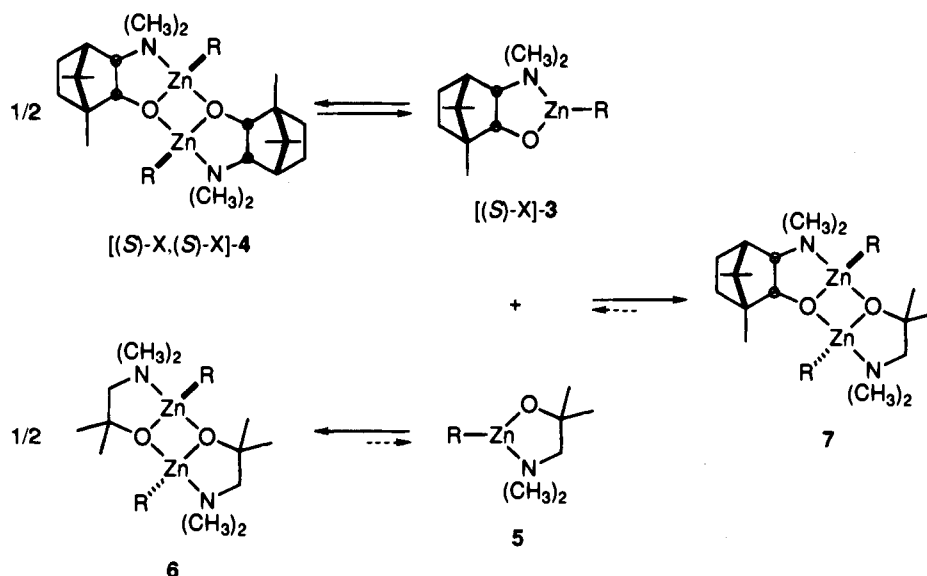


**Figure 13.** Self and nonself recognition of chiral and achiral catalysts, [(S)-X]-3 and 5.

spectrum was consistent with the reported one.<sup>18</sup> In a similar way, pure [(S)-N]-1 was prepared in 19% total yield from (1S)-camphor:  $[\alpha]_D^{20} -36.5$  (*c* 1.52, ethanol). The enantiomeric purities of [(R)-N]-1 and [(S)-N]-1 were confirmed by HPLC analysis of the *N*-3,5-dinitrophenylcarbamates (column, Sumitomo Chemical Co. SUMIPAX OA-4000; eluent, 99.5:0.5 hexane-ethanol mixture; flow rate, 1.0 mL/min; detection, 254-nm light;  $t_R$ , 25.9 min (carbamate from [(S)-N]-1) and 36.1 min (carbamate from [(R)-N]-1)).

**Typical Procedure for Asymmetric Alkylation.** The procedure for the asymmetric alkylation was exemplified using a 60:40 [(S)-X]-1/[(R)-N]-1 system where the concentrations of the mixed amino alcohols, diethylzinc, and benzaldehyde were adjusted to 34, 420, and 420 mM, respectively. The 0.100 M toluene solutions of [(S)-X]-1 (0.902 mL, 0.0902 mmol) and [(R)-N]-1 (0.602 mL, 0.0602 mmol) and toluene (2.03 mL) were placed at 25 °C in a dry argon-filled 20-mL Schlenk tube containing a Teflon-coated magnetic stirring bar. A 2.50 M toluene solution of diethylzinc (0.752 mL, 1.88 mmol) was added at the same temperature. After the solution was stirred for 30 min, during which time ethane gas evolved, the colorless solution was cooled to 0 °C with an ice bath, and benzaldehyde (200 mg, 1.88 mmol) was added. For introduction of the amino alcohols, diethylzinc, and benzaldehyde, gas-tight syringes were used. After 12 h stirring at 0 °C, the mixture was quenched with a saturated  $\text{NH}_4\text{Cl}$  solution (1 mL), and extracted three times with ether (15 mL). The combined organic layers were washed with 1 M aqueous HCl solution (15 mL), water (15 mL), and brine (15 mL), dried over anhydrous  $\text{Na}_2\text{SO}_4$ , and concentrated under reduced pressure to give a yellow oil, which was then chromatographed on a short silica-gel column (1:1 ether-hexane). The yield of 1-phenyl-1-propanol was determined to be 87% by GC analysis (capillary column, GL Science OV-1 0.25 mm  $\times$  50 m; column temperature, 90 °C; rate of temperature increase, 2 °C/min; carrier gas, He; flow rate, 50 mL/min; split ratio, 40:1;  $t_R$  of benzaldehyde, 9.5 min;  $t_R$  of 1-phenyl-1-propanol, 17.2 min). The ee of the product was determined to be 98% by HPLC analysis (column, Daicel Co. CHIRALCEL OB; eluent, 100:0.5 hexane-2-propanol; flow rate, 1.0 mL/min; detection, 254-nm light;  $t_R$  of (*S*)-1-phenyl-1-propanol, 20.1 min;  $t_R$  of the *R* isomer, 25.4 min). The data from the asymmetric alkylation experiments using mixed amino alcohols systems are listed in order of the ratio of the amino alcohols, % yield, % ee, and the absolute configuration of the product. [(S)-X]-1/[(R)-N]-1 system: 100:0, 87, 98, *S*; 80:20, 86, 97.7, *S*; 60:40, 87, 97.7, *S*; 55:45, 85, 90.7, *S*; 50:50, 85, 13.8, *R*; 45:55, 87, 89.1, *R*; 40:60, 80, 93.8, *R*; 20:80, 87, 94.9, *R*; 0:100, 85, 94.1, *R*. [(S)-X]-1/[(S)-N]-1 system: 100:0, 87, 98, *S*; 80:20, 86, 96.4, *S*; 66.7:33.3, 87, 96.5, *S*; 50:50, 85, 97.2, *S*; 33.3:66.7, 87, 96.2, *S*; 20:80, 87, 95.3, *S*; 0:100, 85, 94.1, *S*. [(S)-X]-1/2 system: 100:0, 87, 98, *S*; 80:20, 85, 97.4, *S*; 60:40, 83, 97.4, *S*; 50:50, 85, 96.7, *S*; 40:60, 81, 92.6, *S*; 20:80, 80, 62.2, *S*.

**Typical Procedure for the Kinetic Experiments.** The procedure and scale for the kinetic experiments were the same as those described

for the asymmetric alkylation. The reaction starting point was set at the time when benzaldehyde was added in one portion. At 3–5 min intervals, a ca. 0.3-mL portion was quickly transferred by a cannula to a vigorously stirring mixture of saturated aqueous 3 M  $\text{NH}_4\text{Cl}$  (1.5 mL) and ether (1.5 mL) at 0 °C. The conversion was determined from the ratio of 1-phenyl-1-propanol and unreacted benzaldehyde by GC analysis of the organic layer. Correlations between time (min) and percent conversion were listed for [(S)-X]-1/[(R)-N]-1, [(S)-X]-1/[(S)-N]-1, and [(S)-X]-1/2 ratios. A 100:0 mixture of [(S)-X]-1 and [(R)-N]-1: (0.5 min, 4.9% conversion), (1, 8.2), (1.5, 12.1), (2, 15.6), (2.5, 18.1), (3, 22.4), (3.5, 26.4), (4, 28.3), (4.5, 30.1), (5, 34.0); 7.0%/min = 2.94 mM/min. An 80:20 mixture of [(S)-X]-1 and [(R)-N]-1: (2, 9.4), (4, 18.2), (6, 26.1), (8, 33.4), (10, 39.6); 3.9%/min = 1.64 mM/min. A 60:40 mixture of [(S)-X]-1 and [(R)-N]-1: (5, 4.1), (10, 9.4), (15, 14.3), (20, 19.2), (30, 26.7), (40, 35.2), (60, 42.5); 0.93%/min = 0.391 mM/min. A 55:45 mixture of [(S)-X]-1 and [(R)-N]-1: (10, 9.5), (20, 15.9), (30, 22.7), (40, 32.3), (50, 38.3), (60, 44.3); 0.75%/min = 0.315 mM/min. A 50:50 mixture of [(S)-X]-1 and [(R)-N]-1: (10, 5.2), (20, 9.7), (30, 14.3), (40, 18.2), (50, 21.9), (60, 24.9); 0.41%/min = 0.172 mM/min. A 45:55 mixture of [(S)-X]-1 and [(R)-N]-1: (5, 9.7), (10, 17.7), (15, 24.7), (20, 30.6), (30, 36.4); 1.5%/min = 0.630 mM/min. A 40:60 mixture of [(S)-X]-1 and [(R)-N]-1: (5, 15.6), (10, 26.0), (15, 36.5), (20, 45.0), (30, 57.4); 2.8%/min = 1.18 mM/min. A 20:80 mixture of [(S)-X]-1 and [(R)-N]-1: (0.5, 4.0), (1, 11.4), (1.5, 19.1), (2, 25.4), (2.5, 32.3), (3, 35.8), (3.5, 41.6), (4, 44.0), (4.5, 48.9), (5, 51.0); 14.3%/min = 6.01 mM/min. A 0:100 mixture of [(S)-X]-1 and [(R)-N]-1: (0.5, 12.3), (1, 21.8), (1.5, 31.8), (2, 39.2), (2.5, 45.3), (3, 50.9); 18.5%/min = 7.77 mM/min. A 100:0 mixture of [(S)-X]-1 and [(S)-N]-1: (0.5, 4.9), (1, 8.2), (1.5, 12.1), (2, 15.6), (2.5, 18.1), (3, 22.4), (3.5, 26.4), (4, 28.3), (4.5, 30.1), (5, 34.0); 7.0%/min = 2.94 mM/min. An 80:20 mixture of [(S)-X]-1 and [(S)-N]-1: (1, 10.5), (2, 18.6), (3, 25.6), (4, 33.9), (5, 39.5); 8.0%/min = 3.36 mM/min. A 66.7:33.3 mixture of [(S)-X]-1 and [(S)-N]-1: (1, 11.3), (2, 20.3), (3, 29.0), (4, 36.7), (5, 42.5); 9.1%/min = 3.82 mM/min. A 50:50 mixture of [(S)-X]-1 and [(S)-N]-1: (1, 14.7), (2, 24.9), (3, 34.6), (4, 43.0), (5, 50.1); 10.2%/min = 4.28 mM/min. A 33.3:66.7 mixture of [(S)-X]-1 and [(S)-N]-1: (0.5, 10.0), (1, 15.5), (1.5, 23.7), (2, 29.4), (2.5, 37.5), (3, 40.7), (3.5, 47.5); 13.8%/min = 5.80 mM/min. A 20:80 mixture of [(S)-X]-1 and [(S)-N]-1: (0.5, 11.4), (1, 17.8), (1.5, 27.0), (2, 32.5), (2.5, 40.3), (3, 43.4), (3.5, 50.1); 15.0%/min = 6.30 mM/min. A 0:100 mixture of [(S)-X]-1 and [(S)-N]-1: (0.5, 12.3), (1, 21.8), (1.5, 31.8), (2, 39.2), (2.5, 45.3), (3, 50.9); 18.5%/min = 7.77 mM/min. A 100:0 mixture of [(S)-X]-1 and 2: (0.5, 4.9), (1, 8.2), (1.5, 12.1), (2, 15.6), (2.5, 18.1), (3, 22.4), (3.5, 26.4), (4, 28.3), (4.5, 30.1), (5, 34.0); 7.0%/min = 2.94 mM/min. An 80:20 mixture of [(S)-X]-1 and 2: (1, 5.7), (2, 11.1), (3, 16.3), (4, 20.9), (5, 25.1), (6, 29.5); 5.32%/min = 2.23 mM/min. A 60:40 mixture of [(S)-X]-1 and 2: (2, 5.8), (4, 13.6), (6, 20.6), (8, 26.5), (10, 32.9), (12, 37.0); 3.42%/min = 1.44 mM/min. A 50:50 mixture of [(S)-X]-1 and 2: (5, 10.3), (10, 23.7), (15, 36.0),

(20, 43.1), (25, 49.9); 2.39%/min = 1.00 mM/min. A 40:60 mixture of [(S)-X]-1 and 2: (3, 3.6), (6, 10.4), (9, 15.3), (12, 21.4), (15, 26.8), (18, 30.6); 1.74%/min = 0.731 mM/min. A 20:80 mixture of [(S)-X]-1 and 2: (5, 2.7), (10, 6.3), (15, 9.8), (20, 12.7), (25, 16.1), (30, 20.0); 0.665%/min = 0.279 mM/min. A 0:100 mixture of [(S)-X]-1 and 2: (10, 1.6), (20, 4.7), (30, 7.6), (40, 9.3), (50, 11.0), (60, 13.1); 0.208%/min = 0.0875 mM/min.

**Cryoscopic Measurement.** The number-average molecular weights of the organozinc complexes were determined using a cryoscopic apparatus consisting of an inner cell with an inside diameter of 3 cm and an outer air jacket with an inside diameter of 4.5 cm, which prevents overcooling of the solution. The inner sample cell was equipped with a Beckmann thermometer and a side arm connected to the vacuum-argon line. Through the side arm the cell could be evacuated, filled with argon, and later flushed with argon, while solutions or solids were being added. Molecular weight was calculated in each case from the following:  $\Delta T = K_f \omega / MW$ , where  $\Delta T$  = freezing-point depression (degrees),  $K_f$  = molal depression of the solvent,  $\omega$  = weight (g) of solute in 1000 g of solvent, and MW = molecular weight. The  $K_f$  value was calculated to be 5.16 based on the depression of naphthalene (118.6–566.6 mg) by a benzene (10.53 g) solution. The general procedure for cryoscopic measurement can be illustrated using the complex prepared from [(S)-X]-1 and [(R)-N]-1 in a 1:1 molar ratio. A dried inner cryoscopy cell was replaced, under an argon stream, with [(S)-X]-1 (221 mg, 1.12 mmol), [(R)-N]-1 (221 mg, 1.12 mmol), and benzene (23.4 g). Diethylzinc (1.05 mL of a 2.14 M solution in benzene) was added. After the mixture was stirred at 25 °C for 30 min, the resulting methane gas was removed by three freeze-thaw cycles, and the cell was filled with argon. The cryoscopic apparatus was immersed into an ice-salt bath, and the temperature was measured by a Beckmann thermometer at 30-s intervals until the solution froze. After warming up to room temperature, the same procedure was repeated three times. Since the  $\omega$  value of the benzene solution of [(S)-X,(R)-N]-4 was 27.9 and the averaged  $\Delta T$  value obtained from the three runs was 0.263 (0.262–0.264), the molecular weight (MW) of this compound was calculated to be 546 (544–548).

The molecular weights of the complexes prepared from a 1:1 mixture of [(R)-N]-1 and diethylzinc, from a 1:1:2 mixture of [(S)-X]-1, [(S)-N]-1, and diethylzinc, from a 1:1 mixture of 2 and diethylzinc, and from a 1:1:2 mixture of [(S)-X]-1, 2, and diethylzinc were determined in a similar way. The experimental parameters were as follows. [(R)-N]-1/(C<sub>2</sub>H<sub>5</sub>)<sub>2</sub>Zn system:  $K_f$  5.16;  $\omega$  25.8;  $\Delta T$  0.234 (0.233–0.235); MW 568 (566–571). [(S)-X]-1/[(S)-N]-1/(C<sub>2</sub>H<sub>5</sub>)<sub>2</sub>Zn system:  $K_f$  5.16;  $\omega$  30.5;  $\Delta T$  0.297 (0.294–0.309); MW 530 (510–549). 2/(C<sub>2</sub>H<sub>5</sub>)<sub>2</sub>Zn system:  $K_f$  5.16;  $\omega$  18.3;  $\Delta T$  0.231 (0.225–0.235); MW 410 (403–421). [(S)-X]-1/2/(C<sub>2</sub>H<sub>5</sub>)<sub>2</sub>Zn system:  $K_f$  5.16;  $\omega$  42.4;  $\Delta T$  0.443 (0.440–0.445); MW 494 (491–497).

**X-ray Crystallographic Analysis of [(S)-X,(R)-N]-4, 6, and 7.** The dinuclear zinc complex [(S)-X,(R)-N]-4 was prepared as follows. The amino alcohols, [(S)-X]-1 (90.7 mg, 0.460 mmol) and [(R)-N]-1 (90.7 mg, 0.460 mmol), and toluene (6 mL) were placed in a dry 20-mL Schlenk tube. To this was added a 4.18 M toluene solution of dimethylzinc (0.219 mL, 0.920 mmol) at 25 °C. The resulting white suspension was refluxed for 1 min to give a clear solution, which was cooled to 25 °C in air. After several hours [(S)-X,(R)-N]-4 was precipitated from the solution. Separation of the crystals by removing the supernatant with a cannula was followed by washing twice with cold toluene, and drying under reduced pressure to give colorless prismatic crystals of [(S)-X,(R)-N]-4: <sup>1</sup>H NMR (400 MHz, toluene-*d*<sub>8</sub>, 10 mM at 25 °C)  $\delta$  -0.33 (s, 3, ZnCH<sub>3</sub>), -0.16 (s, 3, ZnCH<sub>3</sub>), 0.91–1.03 (m, 2, 2 CHH), 0.94 (s, 3, CH<sub>3</sub>), 1.07 (s, 6, 2 CH<sub>3</sub>), 1.15–1.34 (m, 2, 2 CHH), 1.18 (s, 3, CH<sub>3</sub>), 1.28 (s, 3, CH<sub>3</sub>), 1.39 (s, 3,

CH<sub>3</sub>), 1.55–1.68 (m, 3, CH and 2 CHH), 1.74–1.86 (m, 1, CH), 1.92 (d, 1,  $J$  = 4.9 Hz, CH), 1.94–2.05 (m, 1, CHH), 2.22 (s, 3, NCH<sub>3</sub>), 2.25 (s, 3, NCH<sub>3</sub>), 2.40–2.52 (m, 1, NCH), 2.44 (s, 3, NCH<sub>3</sub>), 2.53 (s, 3, NCH<sub>3</sub>), 2.58 (dm, 1,  $J$  = 7.3 Hz, NCH), 4.32 (d, 1,  $J$  = 7.3 Hz, 2 CHO); <sup>13</sup>C NMR (100 MHz, toluene-*d*<sub>8</sub>, 10 mM at 25 °C)  $\delta$  -18.3, -16.8, 12.0, 14.9, 19.5, 20.3, 20.6, 22.7, 23.3, 26.8, 29.7, 33.3, 43.3, 44.4, 45.5, 45.9, 48.2, 48.6, 48.9, 50.0, 50.9, 51.0, 70.2, 76.1, 78.4, 84.4; sublimation > 140 °C (0.04 mmHg). Colorless prismatic crystals of 6 and 7 were obtained by setting aside the hexane solution, prepared in a similar way to that for [(S)-X,(R)-N]-4, for 1 day at 25 °C. 6: <sup>1</sup>H NMR (400 MHz, toluene-*d*<sub>8</sub>, 20 mM at 25 °C)  $\delta$  -0.20 (s, 3, ZnCH<sub>3</sub>), 1.44 (s, 6, 2 OCCH<sub>3</sub>), 2.34 (s, 2, NCH<sub>2</sub>), 2.38 (s, 6, 2 NCH<sub>3</sub>); <sup>13</sup>C NMR (100 MHz, toluene-*d*<sub>8</sub>, 20 mM at 25 °C)  $\delta$  -13.5, 31.0, 49.3, 71.4, 73.5; sublimation > 70 °C (0.04 mmHg). 7: <sup>1</sup>H NMR (400 MHz, toluene-*d*<sub>8</sub>, 20 mM at 25 °C)  $\delta$  -0.27 (br s, 3, ZnCH<sub>3</sub>), -0.20 (br s, 3, ZnCH<sub>3</sub>), 0.91–0.99 (m, 1, CHH), 0.93 (s, 3, CH<sub>3</sub>), 1.15–1.30 (m, 1, CHH), 1.26 (s, 3, CH<sub>3</sub>), 1.36 (s, 3, CH<sub>3</sub>), 1.40 (s, 3, OCCH<sub>3</sub>), 1.48 (s, 3, OCCH<sub>3</sub>), 1.55–1.62 (m, 1, CHH), 1.72–1.86 (m, 1, CHH), 1.91 (d, 1,  $J$  = 4.4 Hz, CH), 2.22 (d, 1,  $J$  = 13.2 Hz, NCH<sub>A</sub>H<sub>B</sub>), 2.24 (s, 3, NCH<sub>3</sub>), 2.28 (d, 1,  $J$  = 7.3 Hz, NCH), 2.31 (s, 3, NCH<sub>3</sub>), 2.44 (s, 3, NCH<sub>3</sub>), 2.51 (s, 3, NCH<sub>3</sub>), 2.59 (d, 1,  $J$  = 13.2 Hz, NCH<sub>A</sub>H<sub>B</sub>), 4.29 (d, 1,  $J$  = 7.3 Hz, CHO); <sup>13</sup>C NMR (100 MHz, toluene-*d*<sub>8</sub>, 20 mM at 25 °C)  $\delta$  -18.8, -9.9, 12.0, 22.5, 23.3, 29.8, 30.2, 31.4, 33.1, 44.6, 46.0, 48.2, 48.9, 49.8, 50.1, 51.5, 71.2, 72.6, 78.5, 85.7; sublimation > 80 °C (0.04 mmHg).

**Appendix.** The calculated curves in Figure 7, 10, and 12 were drawn using the following equations.

$$v_0(\text{calcd}) = \frac{v_{0A}[\text{catA}] + v_{0B}[\text{catB}]}{[\text{catA}] + [\text{catB}]}$$

$$ee(\text{calcd}) = \frac{ee_A v_{0A}[\text{catA}] + ee_B v_{0B}[\text{catB}]}{[\text{catA}] + [\text{catB}]}$$

In the equations  $v_{0A}$  and  $v_{0B}$  are the initial rates of the pure catA- and catB-catalyzed reactions which proceed with the enantioselectivities of  $ee_A$  and  $ee_B$ , respectively. Graphic expression of the mathematical equations in Figures 7, 10, and 12 was aided by the Mathematica program on an Apple Macintosh computer.

**Acknowledgment.** We thank Professor H. Suga of Osaka University for suggestions and encouragement. We also acknowledge Dr. T. Ikariya, ERATO Molecular Catalysis Project, Research Development Corporation of Japan, for valuable contributions in the X-ray crystallographic analysis of [(S)-X,(R)-N]-4. This work was aided by the Ministry of Education, Science and Culture, Japan (Nos. 05554016 and 06242208).

**Supplementary Material Available:** ORTEP drawings with numbering scheme, crystallographic data, tables of atomic parameters, anisotropic temperature factors, and complete listings of bond angles and distances for [(S)-X,(R)-N]-4, 6, and 7 (15 pages). This material is contained in many libraries on microfiche, immediately follows this article in the microfilm version of the journal, can be ordered from the ACS, and can be downloaded from the Internet; see any current masthead page for ordering information and Internet access instructions.

JA950012Y